Photonic Propulsion: an Option for Space Resources Transportation to and from the Main Belt

F. DALLA VEDOVA[a,**], N. MIGUEL[b], C. COLOMBO[b]

[a]*LuxSpace, Betzdorf, Luxembourg*
[b]*Dept. of Aerospace Science and Technology, Politecnico di Milano, Italy*

Abstract

With the recent interest for Space Resource Mining (SRM) some key questions could now be anticipated by future "Space Miners" to Photonic Propulsion Experts:

Q1: Shall we consider Photonic Propulsion for future (regular) transportation of Space Resources from the Main Belt (where resource loading will take place) back to Mars, Moon and/or Earth (where unloading will take place)?
Q2: Could we then take benefit of Photonic Propulsion to achieve with one Sailcraft repeated round trips from the Main Belt back to Mars, Moon and/or Earth for regular load/unload cycles?
Q3: Would these Photonic Propulsion based round trips compete with respect to similar supported by Classical Propulsions?

The paper answers these questions for future "Space Miners" allowing them to consider Photonic Propulsion for Space Resource Businesses. The paper assesses current solar sail technologies and required advances enabling such missions, and analyses sail-propelled trajectories for "Stopover Cyclers" for Space Logistics to and from the Main Belt.

Keywords: SpaceResources.lu, Space (Resource) Mining, Space Logistics, Sail Trailer, Stopover Cyclers

Nomenclature

A/M	(Sail) Area-to-Mass ratio [m^2/kg]
A	Sail (Trailer) Area [m^2]
M	Mass [kg]
S	(Square) Sail Sidelength [m]
Superscripts	
T	transposed
Subscripts	
L/UL	Loaded/UnLoaded
RM	Max carriable (Space) Resource Material
SA	Sail Assembly (or Module)
SB	Sailcraft Bus (or Service Module)
ST	SailTrailer

1. Introduction

Solar Sail Trailers (or *Cargo*, or also *Shuttle*) are solar sailcrafts which primary mission is to transport goods through Space thanks to photonic propulsion.

The concept of (Solar) *SailTrailer* is not new [1] but the recent interest for Space Resources (Mining), especially in Luxembourg [2], deserves this new assessment of SailTrailers capabilities as "Stopover Cyclers" [3] for the transport and transfer of Space Resources [4] collected in the Asteroids Main Belt.

This paper intends helping future "Space Miners" in raising their knowledge about photonic propulsion and thus, in supporting their decision to use (or not) photonic propulsion for Space Resource Businesses.

1.1. Introduction on Space Resources (Business)

The Government of Luxembourg decided recently to engage definitely in and foster the "*peaceful exploration and sustainable utilization of space resources for the benefit of humankind*". In support of this vision and in the context of its "**SpaceResources.lu**" initiative, a study [2] has been conducted for the Luxembourg Space Agency (LSA) to identify "*Opportunities for Space Resources Utilization – Future Markets & Value Chains*".

The study concluded in December 2018 that over the 2018-2045 period, the "*Space Resource Utilization industry […] is expected to generate a market revenue of 73 to 170 B€ (Present Value 2018)*" and also that the "*Off-Earth population growth [is expected] to reach a total of several dozen by 2045*". "*The process of*

** Corresponding author, dallavedova@luxspace.lu

populating Mars is predicted to evolve very rapidly to many tens of people in the 10 to 15 years after the first settlers arrive".

Taking this challenging vision as potential application for future SailTrailers, the following sub-sections introduce respectively:

- The envisaged locations in space where space resource mining/utilization will take place,
- The considered valuable space resource materials, proposed to be transported between the envisaged locations.

1.1.1. Envisaged Locations

When considering space resources (utilization), investigations and sky surveys identified so far the following locations / steps:

1. **Moon**, as first "play-ground" especially for surface operations (see Apollo missions, *50 years ago !*),
2. **Space Stations** (Mir, ISS, Tiangong) as second "play-ground", especially for rendez-vous, docking/berthing and material transfer operations,
3. **Near-Earth Asteroids (NEAs)**, as third "play-ground", especially for navigation to/from, landing or impact, then departure operations,
4. **Mars**, as fourth "play-ground", replicating Moon operations, still somewhat farther in our Solar System,
5. **Main Belt** (see next Fig. 1), as final "field of operation" because location of the most valuable asteroids.

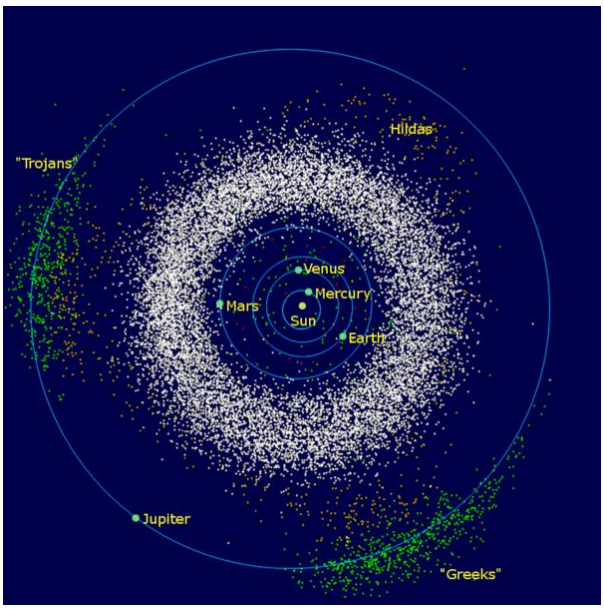

Fig. 1. The inner Solar System, from the Sun to Jupiter showing with white dots representing asteroids, **the Main Belt** orbiting around the Sun (in ≈ [1.7 ; 4.5] AU) between Mars (1.52 AU) and Jupiter (5.20 AU) [5],[6].

As seen on Fig. 2, most valuable asteroids are indeed to be found in the Main Belt "*far from Earth*" [7] at minimum distances (from Earth) between 1 and 2 AU:

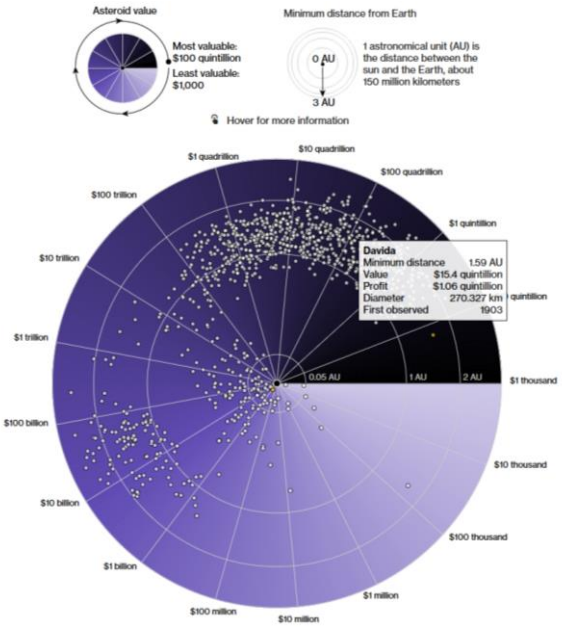

Fig. 2. "*Most valuable asteroids are far from Earth*" [7]. The most valuable asteroids orbit at minimum distances from Earth between approximately 1 and 2 AU. The 10 most valuable asteroids (including Davida) in fact orbit at minimum distances from Earth between 0.805 and 2.790 AU.

Integrating the information collected in Fig. 1 and 2 leads to the definition with the subsequent Fig. 3, of the "*Most Valuable Field of Operation*" for asteroid mining in the Main Belt:

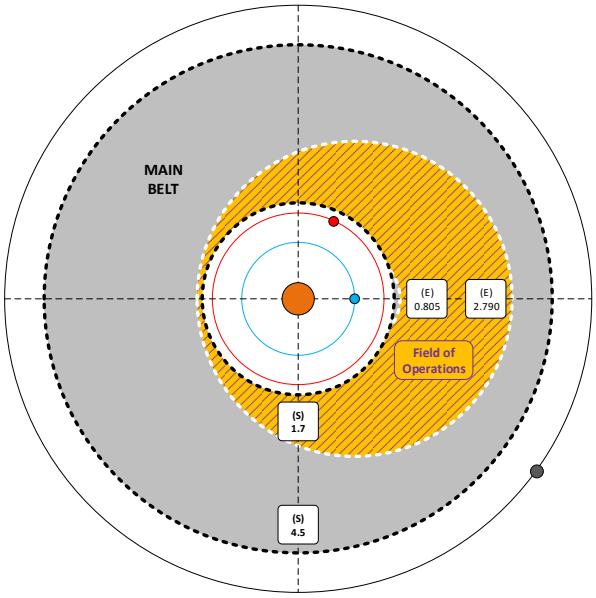

Fig. 3. The "*Most Valuable Field of Operations*", integrating all Sun- (in orange) and Earth- (in blue) centred distances identified in Fig. 1 and Fig. 2.

From the Main Belt, space resources are planned to be shipped back to/around Mars, the Moon (proximity) and even down to the Earth surface. The main question posed in this paper is thus: *"How to perform efficiently the various and repeated interplanetary journeys that will be necessary for space resource utilization between the Main Belt and ultimately the Earth ?"*

1.1.2. Valuable (Space) Resources

Although asteroids characterisation is still far from being exhaustive and detailed to the needed level, the first value chains for space resources have already been identified [2] and mainly relate to:

- **Water** (for in-space propulsion and life support)
- **Regolith and Metals** (for in-space construction and manufacturing)
- **Highly-valuable Metals** (to bring back to Earth Surface)

The following figure, extracted from [2] presents the roadmaps of these space resources value chains:

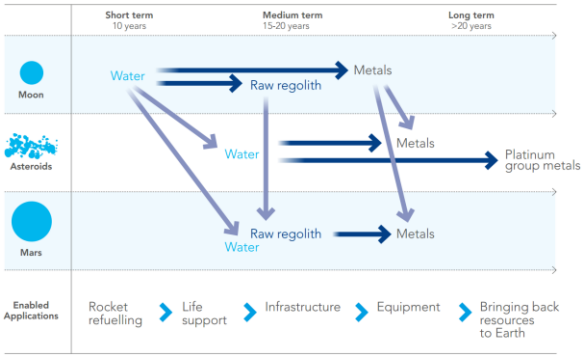

Fig. 4. Roadmap of space resources value chains developments (extracted from [2]). For the scope of this paper, it is worth noting that "*Long term" should become reality after 2038.*

1.2. Possible Questions from Future "Space Miners"

With the intention to help future "Space Miners" in raising their knowledge about photonic propulsion and thus, in supporting their decision to use (or not) photonic propulsion for space resource businesses, some first possible "Space Miners" questions to Photonic Propulsion Experts could here be anticipated. "Space Miners" could indeed ask:

- **Question Q1**: "*Shall we consider photonic propulsion for future (regular) transportation of space resources from the Main Belt (where resource loading will take place) back to Mars, Moon and/or Earth (where unloading will take place) ?*"

  The subsequent sections **will answer positively** to this question underlining the need for this to continue improving the sailcraft technologies and (areal) performances.

- **Question Q2**: "*Could we then take benefit of photonic propulsion to achieve with one sailcraft repeated round trips from the Main Belt back to Mars, Moon and/or Earth for regular load/unload cycles ?*"

  The subsequent sections **will answer positively** to this question showing that SailTrailers, repeating Stopover Cycles between Starting and Target locations, will be able to perform this task until their disposal.

- **Question Q3**: "*Would these photonic propulsion based round trips compete with respect to similar supported by classical propulsions ?*"

  Due to today's lack of information regarding development costs of futuristic, advanced SailTrailers, the subsequent sections **will only provide a partial but a priori positive answer** to this question reminding that the SailTrailers here defined would travel (on average) as fast as past inter-planetary space probes (all using classical propulsion) and this, without any classical propulsive equipment nor propellant (refuellings) to perform their repeated Space Logistic mission.

1.3. Introduction on Resources Mining (Processes)

Space resources mining (processes) will very probably show large similarities with Earth resources mining (processes). The following two examples of related Earth-based extractive processes should thus allow the understanding of which are the necessary processes and where they could optimally be performed in Space.

1.3.1. Gold Processes – Example (proposed) in French Guyana

The example of the "Montagne d'Or" project relates to a possible open-air/open-pit gold mine in French Guyana. This (future?) project is currently being discussed in France up to Presidential level [8],[9],[10].

In brief (and in numbers) the "Montagne d'Or" project will extract gold by crushing and then washing (with cyanide) rocks containing the precious resource. It is here expected in 12 years operations to:

- Dig a 2.5 (long), 0.12 (wide), 0.4 (deep) km mine,
- Extract from there ultimately 85 tons of gold,
- Require for this (over 12 years):
  - 57 154 tons of explosives,
  - 2 200 trucks movements per day,
  - 142 million of litres fuel,
  - 20 MW of electrical power supply,
  - 66 000 tons/day of rock waste,

- 12 500 tons/day of treatable rock,
- 46 573 tons of cyanide.

1.3.2. Nickel Processes – Example in New Caledonia

From ground to metal, Nickel (in New Caledonia) requires at least 11 processes [11],[12],[13]:

1. Sounding/sampling ("*sondage*") to characterise and confirm interest for the future mining site,
2. Scraping ("*décapage*") to remove the first, upper layers of natural ground for later re-use in site restoration,
3. Extraction ("*extraction*") for operational collection of the valuable rocks containing Nickel,
4. Sorting ("*tri*") to crush and separate valuable rocks from unvaluable residuals,
5. Transport to sea ("*expedition au bord de la mer*") to transport valuable ore ("*minerai*") by ships to storage and treatment sites,
6. Unloading ("*déchargement du minerai*") to unload the ships and store the ore in heaps,
7. Homogeneization ("*homogénéisation du minerai*") to homogenize the Nickel content in the storing heaps,
8. Pre-drying ("*préséchage*") to remove excessive moisture in ore hence reduce electrical power consumption in subsequent step,
9. Calcination ("*calcination du minerai*") to remove by combustion (flames) the last traces of water content and pre-heat the metallic oxides,
10. Electrical fusion/reduction ("*fusion du minerai*") to retrieve the raw Ferronickel product,
11. Refining ("*affinage des ferronickels*") to de-sulphidize the raw ferronickel product and obtain the final product in its commercial form: the Nickel shots.

These processes are in-line with the typical, high-level processes used in **Extractive Metallurgy** [14]:

1. **Mineral processes**, aiming at transforming the extracted, "run of mine" rocks into valuable (concentrated) material to be subjected to subsequent metallurgical processes. Mineral processes include the sequence of:
    a. **Comminution processes**, aiming at reducing up to granular (i.e. mm / μm) size the "run of mine" materials, and,
    b. **Concentration processes**, aiming at sorting and concentrating the ore.
2. **Metallurgy processes**, aiming at transforming the valuable material coming from the mineral processes in commercial/final metal products. Metallurgy processes implement only one or a combination of both type of:
    a. **Pyrometallurgy processes**, using thermal treatments and/or,
    b. **Hydrometallurgy processes**, using electro-chemical (including electrolysis) treatments.

Should we transpose these Extractive Metallurgy processes into Space, then the following guiding principles for identifying optimal locations in space for those necessary processes could apply:

- Leave non-valuable material closest to its extractive site,
- Move in/through Space only valuable material,
- Value of the processed/transported material shall increase with decreasing distance to its final destination,
- Remember that photovoltaic electric power production is more effective when performed closer to the Sun.

1.4. Elements of Benchmarking with Classical Inter-planetary Propulsion

The advent of IKAROS in 2010 opened the way for inter-planetary missions supported by photonic propulsion. *So far <u>all</u> inter-planetary space probes used classical (i.e. chemical and/or electrical) propulsion.*

The current plans for in-orbit resources exploitation also for sure consider classical propulsion as main enabling technology, especially if itself based in the future on space resources for propulsion like water and/or methane.

To support the comparison of propulsive technologies (i.e. photonic vs. classical) a benchmarking exercise has been performed for this paper. Data from 19 successful inter-planetary missions (most of them targeting Mars or Jupiter) and their respective space probes has been collected (mainly from NASA's Press Kits) and analysed.

The three following sub-sections present the outcome of the benchmarking analysis respectively for:

- Travel time/duration
- Wet-to-Dry mass ratio
- Mission cost

1.4.1. Travel Time

The <u>time needed to travel from Earth</u> to whatever planet in the Solar system depends heavily on the mission, i.e. from choices like e.g. launcher capability, launch window and number of flybys.

It is however commonly accepted and confirmed by the analysis made for this study that:

- An **Earth-to-Mars** journey (i.e. radially: 0.52 AU) varies between 6 to 8 months. The analysis of 7 missions heading Mars led to:
    - Min: 0.46 yrs (Mariner 9)
    - **Average duration: 0.63 yrs or 7.6 months**
    - **Average speed: 0.52/0.63 = 0.82 AU/yr**

    - Max: 0.84 yrs (MAVEN)
- An **Earth-to-Jupiter** journey (i.e. radially: 4.20 AU) varies between 2 to 8 years. The analysis of 5 missions heading Jupiter led to:
    - Min: 1.11 yrs (New Horizons)
    - **Average duration: 4.31 yrs**
    - **Average speed: 4.20/4.31 = 0.97 AU/yr**
    - Max: 7.60 yrs (JUICE)

Based on these, the average (radial) speed of 0.895 AU/year was considered in the following for comparisons between classical vs photonic propulsions.

1.4.2. Wet-to-Dry Mass Ratio of Space Probes

The analysis of Wet and Dry mass data of 12 successful inter-planetary space probes led to the following numbers for Wet/Dry mass ratio:

- Min: 1.12 (Voyager 1)
- **Average: 1.97**
- Std Deviation: 0.61
- Max: 3.03 (MAVEN)

As can be seen from these numbers, it is typical that propellants account for almost the same mass as the dry space probe itself ! *What if, thanks to photonic propulsion, all or part of this (propellant) mass fraction could be profitably substituted by valuable space resources instead ?*

1.4.3. Inter-Planetary Missions (and other relevant) Costs

The analysis of mission costs data of 9 successful inter-planetary missions led to the following numbers when reported to:

- Launched **WET** space probe mass:
    - Min: 0.27 M$/kg (MAVEN)
    - **Average: 0.53 M$/kg**
    - Std Deviation: 0.37 M$/kg
    - Max: 1.46 M$/kg (New Horizons)
- Launched **DRY** space probe mass:
    - Min: 0.63 M$/kg (Dawn)
    - **Average: 0.97 M$/kg**
    - Std Deviation: 0.36 M$/kg
    - Max: 1.74 M$/kg (New Horizons)

Two other costs are inserted here because of their relevance to this paper:

- **Cost of ISS** [15]: since 1985 and up to 2015, 150 Billions $(2010) have been spent by the USA and the other partnering Nations for this ultimately 304 tons manned-space infrastructure orbiting around the Earth. Cost of ISS resulted thus (also) to be about *Half a Million of $(2010) per Kilogram in Low Earth Orbit (LEO).*
- **Cost of MiNEOs** [16]: A 3-months challenging Space Mission Analysis and Design (Phase 0/A) exercise performed by a team of 11 Students of the Politecnico di Milano investigated the mission elements required for mining and repeatedly transport space resources from the Nereus NEA for in-orbit storage in Earth-Moon environment. The ideated MiNEOs mission, estimated at 3900 MEuro (2029), would be launched in 2031 and last up to 2060 to bring back in five shipments *up to 3 tons of collected raw metallic material*. MiNEOs would need for this, five different space modules and would need to install/operate in space 6.4 tons (dry) / 20.8 tons (wet) of hardware. If confirmed, MiNEOs costs would thus lead to the following numbers when reported to:
    - Launched **WET** H/W mass: **0.19 M€/kg**
    - Launched **DRY** H/W mass: **0.61 M€/kg**

2. Simulations Framework

In order to provide the promised answers to the "Space Miners" potentially interested in SailTrailers for Space Logistics between Earth and the Main Belt, a plan for dedicated astrodynamic simulations had to be established first.

As this plan required the definition of a Space Logistics scenario and an assessment of future SailTrailer capabilities, these are introduced in the following sub-sections.

2.1. Investigated (Regular) Journeys for Space Logistics

Thanks to the previous, introductive sections it emerges that Space Resource Mining (in the Main Belt) will probably require:

- An initial, step-by-step implementation of the necessary space infrastructure, starting from Earth, e.g. for:
    - Surface or orbital infrastructures for extractive metallurgy processes
    - Ovens operating with flame burners (fuel)
    - Ovens operating with electrical power supply
    - Large (electrical) power generation facilities
- Regular logistic journeys, from Earth to Main Belt, for consumables not producible in space, e.g. (TBC – To Be Confirmed):
    - Explosives
    - Dangerous (contaminating) chemicals
    - Radioactive power sources
- Regular logistic journeys, from the Main Belt to Earth, to bring back the highly valuable space materials.

Thus, even if some of the necessary infrastructure (elements) and/or consumables could one day be produced in space, Space Resource Mining (SRM) will

involve initial and/or regular journeys between Earth and the Main Belt.

Although several destinations/locations have been identified (in section 1.1.1), the analyses performed for this paper focused on Earth-Main Belt operations, with the following scenario:

1. Loading of a SailTrailer with equipment and/or consumables in Earth proximity,
2. Travel towards a major in-space orbiting infrastructure devoted to Space Resource Mining and (part of) its extractive metallurgy processes. Such infrastructure would be assembled and operated at the closest and/or farthest edges of the Main Belt or at those of the Most Valuable Field of Operations,
3. Unloading of Earth-originating equipment and/or consumables,
4. Loading of highly valuable space materials,
5. Travel back to Earth proximity,
6. Unloading of highly valuable space materials,
7. (Cycle repetitions from 1. to 6. until SailTrailer disposal).

Such scenario will thus require repeated and regular journeys for space logistics between Earth and the edges the Main Belt or those of the Most Valuable Field of Operations previously shown in Fig. 3:

Table 1. Investigated Journeys

Journey ID	Starting, wrt Sun (AU)	To, wrt Sun (AU)	Radial Dist. (AU)
J1.7E	Earth (1.00)	1.700	0.700
J1.8E	Earth (1.00)	1.805	0.805
J3.8E	Earth (1.00)	3.790	2.790
J4.5E	Earth (1.00)	4.500	3.500

2.2. SailTrailer Area-to-Mass Ratio Framework

SailTrailers simulations require the identification of current and future SailTrailer's (loaded and unloaded) Area-to-Mass ratio (A/M_{ST}) as key parameter for photonic propulsion.

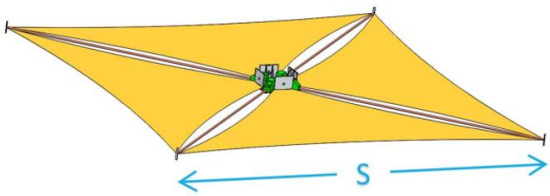

Fig. 5. Sketch of a typical square, four sail segments Sail (Module) defining the sail sidelength "**S**" as the tip-to-tip distance of the ideal square sail.

Considering a SailTrailer "ST" as a typical square sailcraft (see Fig. 5) with sidelength "S", its ideal (maximal) sail area would be:

$$A^* = S^2 \quad (1)$$

However, many of the square sailcraft designs leave void surfaces in the sail plane so that the effective sail area of the SailTrailer is in fact:

$$A = \eta . S^2 \quad (2)$$

Considering a SailTrailer "ST" as a sailcraft, typically constituted of a (square) Sail (Assembly) "SA" Module, as on Fig. 5, and a supporting Service/Bus "SB" Module, carrying or not (Space) Resource Material "RM", the mass of a fully loaded SailTrailer can thus be written as:

$$M_{ST} = M_{SA} + M_{SB} + M_{RM} \quad (3)$$

Considering also that the mass of the Service/Bus Module "SB" is proportional to the mass of the Sail (Assembly) Module "SA" and, that the carried mass of (Space) Resource Material "RM" can range between "empty" and "fully loaded", Eq. (3) becomes:

$$M_{ST}(\alpha, \beta) = (1 + \alpha) . M_{SA} + \beta . M_{RM} \quad (4)$$

The (loaded/unloaded) SailTrailer Area-to-Mass ratio is thus:

$$\frac{A(\eta)}{M_{ST}(\alpha,\beta)} = \frac{\eta . S^2}{(1+\alpha) . M_{SA} + \beta . M_{RM}} \quad (5)$$

In support of two recent ESA projects relating to de-orbiting and risks of collisions with DragSails [17],[18], a survey of Sail (Assembly) Modules masses has been done leading to the following graph:

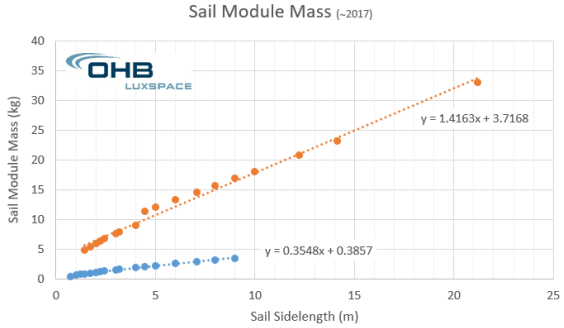

Fig. 6. Sail modules masses (before and around year 2017) are approximately linear functions of (square) sail sidelengths [17],[18]. The graph shows also the importance of boom technology used: Large, Heavy booms (in orange) up to 450 m^2 or Small, Light booms (in blue) up to 86 m^2.

The above Fig. 6 leads to **"Current" Sail Module A/M_{SA} between [0.4 ; 24.5] m^2/kg with an average of 5.0 m^2/kg**, but space resources mining to asteroids in the Main Belt will not start soon and will thus leave some more time to progress on sailcraft technologies. Could we already identify A/M_{SA} targets for future Sail Modules ? The answer is YES considering two sources of information:

- **M. Macdonald and C. McInnes 2004 Roadmap** [19],[20] requesting (in 2004) sailcrafts with deployed sail areas between [1600 ; 76176] m^2, featuring in the:
  - "Near" future: 33 m^2/kg
  - "Mid" future: 100 m^2/kg
  - "Far" future: 667 m^2/kg
- The 2016 ***Breakthrough Starshot Initiative*** **(BSI)** [21] requiring deployed sail areas between [1 ; 314] m^2, featuring 5714 m^2/kg for a TRL 8 in 2049 !

This huge technology step of 3 orders of magnitude can be shown with the following graph, where the collected A/M_{SA} have been replaced by their $Log_{10}(A/M_{SA})$ values:

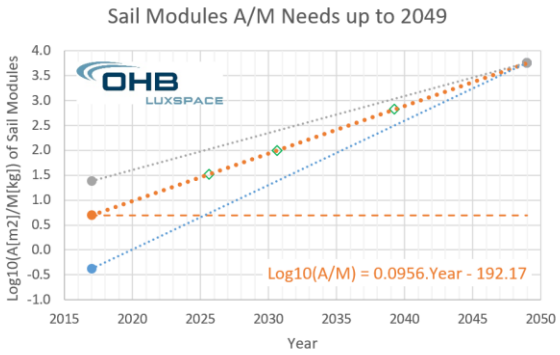

Fig. 7. Needed evolution for Sail Modules A/M_{SA} from 2017 ("Current") up to 2049. Starting from "current" min, average, max capabilities, sail technologies shall progress towards the needs expressed by the Breakthrough Starshot Initiative (BSI).

Eq. (5) can be rewritten as:

$$\frac{A}{M_{ST}} = \frac{1}{\frac{(1+\alpha)}{\theta} + \beta.\frac{M_{RM}}{A}} \tag{6}$$

to better show the inverse effect of loading on cruising performances, and the sole dependence on technologies and system design of the unloaded SailTrailer:

$$\left.\frac{A}{M_{ST}}\right|_{UnLoaded} = \frac{\theta}{(1+\alpha)} = \frac{\eta.S^2}{(1+\alpha).M_{SA}} \tag{7}$$

With these, the relationship between loaded (L) and unloaded (UL) SailTrailer masses can be simplified as:

$$M_{ST}|_L = \left(1 + \beta.\frac{M_{RM}}{M_{ST}|_{UL}}\right).M_{ST}|_{UL} \tag{8}$$

Concluding this section, and for any SailTrailer simulations relating to Space Resource Mining, Eq. (6) can be used to assess current and future, loaded and unloaded SailTrailer A/M_{ST} with:

- **Alpha (α)** depending on SailTrailer functionalities and design, falling historically within [0.04 ; 19.53] with asymmetric distribution characterised by:
  - **Average: 2.23**
  - Standard Deviation: 3.39
  - Skew: 3.09
- **Beta (β)** setting the amount of SailTrailer (space resource material) loading, falling within [0% ; 100%]
- **Eta (η)** as Sail (Assembly) module areal efficiency, and falling historically within [92% ; 100%]
- **Theta (θ)** i.e. A/M_{SA} in [m^2/kg] depending on Sail (Assembly) module technologies at a given date, and derived from the linear (in Log_{10}) interpolations presented in Fig. 7
- **(Space) Resource Loading** M_{RM}/A in [kg/m^2]

3. Trajectory and Mission Design

For the purposes of this paper, the most intuitive trajectory design is that of the so-called "Stopover Cyclers" with Solar Sails [3]. From a generic perspective, Cyclers are a kind of periodic interplanetary trajectories that start and end on the same starting celestial body –typically Earth– and along its way the spacecraft goes through several close encounters between the starting and another target celestial body. In the literature this target body is another planet, usually Mars. The word "Stopover" is added to inquire that between the body-body transfers a waiting time around each of the bodies is considered, where in the context of this contribution the loading and unloading of mining goods is assumed to happen.

In this section, the starting planet (from now on referred to with S) is the Earth, while the target body (referred to as T) is a space infrastructure orbiting close or in the Main Belt. The exposition provided is intended to be general in the sense that the analysis could be easily applied to any body in the Main Belt.

Note that the fact that one assumes waiting times between transfer arcs adds symmetries to the problem that reduce the trajectory design and analysis substantially, namely to the computation of a simple transfer leg, as we justify in the next subsection. These symmetries can also be exploited in the case under study here, where the trajectory to go from S to T is different from the trajectory to go back from T to S as the SailTrailer in the return journey is assumed to be loaded with resource materials that decreases the A/M ratio.

3.1. Models

According to the usual practices in the analysis of Cyclers [22], the starting and target bodies are assumed to be in circular coplanar orbits of radii r_S, r_T that hence have respectively angular velocities

$$\omega_S = \sqrt{\frac{\mu_\odot}{r_S^3}}, \omega_T = \sqrt{\frac{\mu_\odot}{r_T^3}} \tag{9}$$

where $\mu_\odot = 1.32712440018 \times 10^{11} \mathrm{km}^3/s^2$ is the standard gravitational parameter of the Sun. The dynamics of the spacecraft under consideration is also

assumed to be planar, namely here the Solar Radiation Pressure (SRP) perturbed Kepler Problem is considered, whose equations in a heliocentric inertial frame $\mathcal{F}_J$ read

$$\ddot{x} = -\frac{\mu_\odot}{r^3}x + a_{SRP}, \tag{10}$$

where $x = (x, y)^\top, r = \sqrt{x^2 + y^2}$ and a_{SRP} is the acceleration due to SRP. Sailcraft under consideration are assumed here to have an already deployed Solar Sail that consists of a single square flat reflective plate of area A as that in Fig. 5. To avoid out-of-plane motion, the SRP acceleration is assumed to depend solely on a clock angle δ, that measures the angular distance to be exactly perpendicular to the sunlight direction. For practical purposes it is convenient to adimensionalise Eq. (10) by scaling distances and times with factors

$$L = 1\text{AU} \ ; \ T = \sqrt{\frac{L^3}{\mu_\odot}} \approx 5022642.89\text{s}. \tag{11}$$

With this choice, one length unit is 1 AU and a time unit corresponds to approximately 2 months.

3.2. SRP Force Model

Following [23], the force model for SRP applied to the sail plate considers that photons are partially absorbed and partially specularly reflected

$$F = -p_{\text{SR}}A(\text{n} \cdot \text{u}_\text{S})(2\eta(\text{n} \cdot \text{u}_\text{S})\text{n} + (1-\eta)\text{u}_\text{S}), \tag{12}$$

where n is the normal vector to the surface of the plate, u_S is the Earth-Sun vector, η is the (adimensional) reflectance parameter and

$$p_{\text{SR}} = p_{\text{SR at 1AU}}\frac{1\text{AU}^2}{r^2} \tag{13}$$

is the solar radiation pressure. If a clock angle $\delta \in [-\pi/2, \pi/2]$ is introduced, the SRP acceleration reads, in the scaled variables

$$\frac{A}{m}\frac{\text{L}^2\, p_{\text{SR}}}{\mu_\odot \text{r}^2}\begin{pmatrix}\cos\theta + \eta\cos(2\delta+\theta)\\ \sin\theta + \eta\sin(2\delta+\theta)\end{pmatrix}. \tag{14}$$

Here δ is the control variable that will be later used to find time-optimal body-body transfers.

3.3. Stopover Cyclers, Concept and Analysis

A complete period of a stopover cycler consists of four (4) Phases, that can be qualitatively described as follows:

1. $\boldsymbol{S \to T}$: The first phase consists of a transfer from the starting to the target body. This is chosen to be time optimal with δ as control variable.
2. $\boldsymbol{T \to T}$: This second phase consists of a waiting time in the target body intended to be spent in loading the mining goods.
3. $\boldsymbol{T \to S}$: The third phase is the return to the starting planet, with the similar properties of the $S \to T$ phase, and
4. $\boldsymbol{S \to S}$: the fourth and last phase is a waiting time period until the initial conditions of the $S \to T$ phase are recovered so that the cycle can be repeated. This is meant to be used to mainly unload the goods loaded in the $T \to T$ phase.

From a mission analysis perspective, in the classical setting, there are a number of features and symmetries of the problem that can be exploited for the reduction of the computational effort: on the one hand, the period of a whole cycle is a multiple of the synodic period of the target body with respect to the starting one,

$$T_s = \frac{2\pi}{\omega_S - \omega_T}. \tag{15}$$

On the other hand, if the A/M ratio does not change, the $T \to S$ phase has to be symmetric to the $S \to T$ phase, so that the transfer times of the two transfers between bodies are exactly the same. This symmetry has other advantages: the relative position between bodies at the very beginning of the $S \to T$ phase is the ending relative position of the bodies in the final $S \to S$ waiting phase; the absolute value of the angular distance between bodies in the beginning (resp. end) of the $S \to T$ phase is the same as the same quantity in the end (resp. beginning) of the $T \to S$ phase. This reduces the study of the problem to:

1. The choice of the relative initial positions of the bodies, and
2. The choice of the profile of the control angle δ.

This can be easily generalized to the setting faced here, where after the loading process in the $T \to T$ phase the sailcraft has an increased mass of resource materials and hence the overall A/M ratio of the spacecraft is reduced. The exploitation of the symmetries is done via considering transfers $S \to T$ with the A/M ratio as tuning parameter, and later on constructing whole cycler trajectories taking into account that in the $T \to S$ phase the sailcraft mass is higher and hence the A/M ratio is lower.

4. Numerical Study

The assessment of photonic propulsion for prospective mining purposes can be reduced to the study and comparison of circle-to-circle time-optimal trajectories with the aid of SRP acceleration. If this is done considering the A/M ratio as the main tuning parameter of the problem, the results of the sensitivity analysis of transfer times of one single arc – say either an $S \to T$ phase or a $T \to S$ phase – can provide valuable information on two aspects: on the one hand it can inform on ranges of A/M ratio for which such a transfer

is feasible; and on the other hand on the amount of resource materials that can be carried in the way back taking into account the reduction of A/M ratio.

Seeking time-optimal transfers is an optimal control problem that has been treated here using PSOPT (Release 4), an implementation of a direct pseudo-spectral method in the C++ programming languages. Other interesting options that could also be used for the purpose of these contributions are indirect methods as suggested in [24], that first look for adequate initial conditions for the co-state equations using genetic algorithms, that are later refined using gradient-based direct methods.

4.1. Numerical Experiment

As the study to be performed has been reduced solely to the investigation of time-optimal circle-to-circle $S \rightarrow T$ transfers as a function of the A/M ratio of the sail, the only remaining parameter to take into account is the difference in initial phasing between the Earth and the body of the Main Belt to study. After the space and time scaling, one can always choose the x axis of $\mathcal{F}_\mathcal{I}$ in a way that the Earth is initially at $(1,0)^\mathrm{T}$ AU. The target body is assumed to be on a circle of radius R with true anomaly $\Delta\theta_0$, where $\Delta\theta_0 \in [-\pi, \pi]$ rad, see Fig. 8.

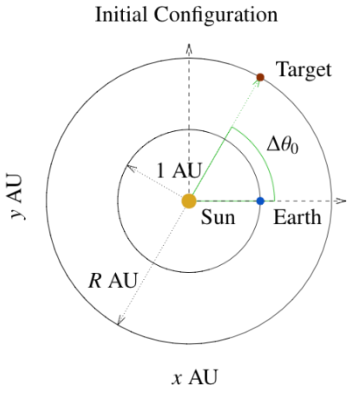

Fig. 8. Sketch of the initial configuration of all numerically computed transfers.

To provide a general perspective on the possible transfers to the Main Belt, four values of the target radius have been proposed in Table 1, two at the inner edges and two at the outer edges of the Main Belt, namely:

$$R = 1.7\ ;\ 1.805\ ;\ 3.790 \text{ and } 4.5 \text{ AU}. \qquad (16)$$

So, the set of results of this study is an assessment of A/M ratio values and $\Delta\theta_0$ that give rise to feasible transfers from 1 AU to any of the radii in Eq. (16). These results are separated in three different aspects: First, transfers for a fixed value of $\Delta\theta_0$ are studied, namely the behaviour of the transfer time for a fixed value of $\Delta\theta_0$ when the A/M ratio varies is explained and exemplified. After this, time optimal transfers with photonic propulsion that can be compared from the point of view of transfer time (or mean radial speed) with already launched and successful probes (see section 1.4.1). This will provide with initial conditions to study how does the transfer time / mean radial speed depend on the A/M ratio of the probes. Finally, the time spans of full cycles will be studied in specific cases of interest.

4.1.1. Time-optimal Transfers for Fixed $\Delta\theta_0$

Assume that we fix an initial $\Delta\theta_0$ for which we can transfer from 1AU to RAU with some value σ of the A/M ratio, with less than one full revolution to Earth's orbit. If we consider variations with respect to σ, one would expect that the larger σ, the shorter the transfer time would be.

As the control we are dealing with is the orientation of the sail with respect to sunlight δ, that is bounded in $[-\pi/2, \pi/2]$, even if σ increases, the control profile has to always take into account the fact that it has to brake to arrive at the sphere of influence of the target planet with its velocity on its orbit. The photonic propulsion thrust cannot be aimed in any direction so even though the radial distance can be covered in less time, the rendezvous to the target body can give rise to a longer transfer time due to some waiting period required for the manoeuvre.

This is exemplified in Fig. 9 for time-optimal transfers to the two examples at the inner edges of the Main Belt, where an initial $\Delta\theta_0 = 60°$ was chosen. Note that there is nothing special about the choice of this value of $\Delta\theta_0$ as the results are only meant to exemplify the phenomena described now. The ordinates range is chosen to show mean radial velocities above the minimum found in previous missions from Earth to Mars with conventional propulsion means: 0.62 AU/y.

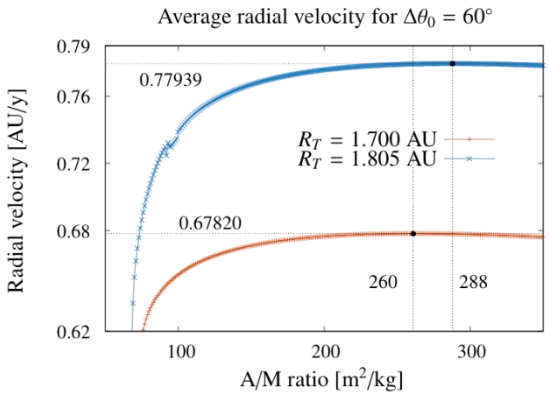

Fig. 9. Mean radial velocities of time-optimal transfers to $R = 1.7$ AU (orange, plus signs) and to $R = 1.805$ AU (blue, cross signs) for transfer orbits with initial $\Delta\theta_0 = 60°$.

On the above graph, it can be seen that required values of σ for such transfers exceed 50 m^2/kg, and that the speed behaviour as σ is increasing is as σ does, reaches a maximum, and then starts decreasing. In the plot the maxima are indicated using a dot on the continuation curves and dotted lines to guide. For the transfers to $R = 1.7, 1.805$ AU, the maxima are attained at approximately 260 and 288 m^2/kg with mean radial velocities of 0.67820 and 0.77939 AU/y, respectively. One can see that on the blue (crossed) curve there seems to be a discontinuity. This is mainly because PSOPT finds a locally optimal solution and the process can converge on orbits (transfers) of different families, meaning that the shape is qualitatively different. This phenomenon will be observed in the forthcoming numerical results, mainly as R increases, and it will be exemplified later.

It is worth noting that the radial velocities for smaller values of the A/M ratio are substantially smaller as they eventually require to perform complete turns around the orbit of the Earth before arriving at the target body.

4.1.2. Time-optimal Transfers with Free $\Delta\theta_0$

The results of the previous sub-section suggest that the strategy for finding time-optimal transfers as continuation of previous computations, as those found for Fig. 8, is to allow $\Delta\theta_0$ to be chosen by the optimizer, and then continue the obtained solutions with respect to $\Delta\theta_0$ in case of interest.

This study focuses in transfers that can compete with classical propulsion means, that is, in transfers from 1 AU to either 1.7 or 1.805 AU whose radial velocity is between 0.62 and 1.13 AU/y (inner Main Belt), and in transfers from 1 AU to either 3.790 or 4.5 AU whose radial velocity is between 0.55 and 3.82 AU/y (outer Main Belt). In Fig. 10 Top, the mean radial velocities of time-optimal transfers for the 4 target radii of interest are displayed in the range of velocities of interest to transfer to the inner Main Belt, the velocities to reach 3.790 and 4.5 AU being added solely for comparison. The Bottom graph displays the corresponding initial $\Delta\theta_0$ chosen by the optimizer.

In both Top and Bottom graphs one observes the change of family of solutions as jump discontinuities in the continuation curves already discussed above. This behaviour appears mostly in transfers to the outer edge of the Main Belt, as the transfer time is larger and more locally optimal solutions with the same constraints can be found. The fact that the family of solutions is different can be also seen in the corresponding sudden change of $\Delta\theta_0$ below.

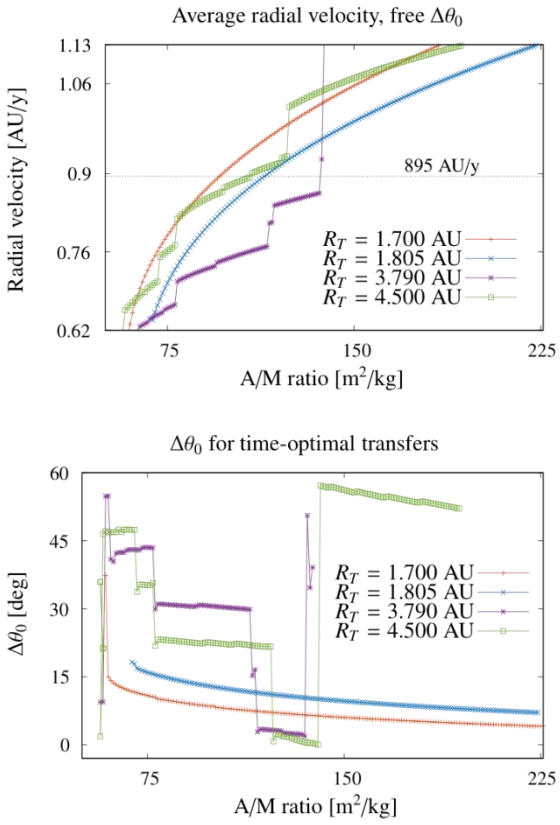

Fig. 10. Top: Mean radial velocity of time-optimal transfers from Earth to $R = 1.7$; 1.805 ; 3.790 and 4.5 AU. Bottom: Initial corresponding $\Delta\theta_0$ of the time-optimal transfers of the Top graph.

Fig. 11 contains analogous information but for transfers from Earth to the outer Main Belt, in the range of radial velocities above 0.55 AU/y. The Top graph informs about radial velocities of optimal transfers as a function of the A/M ratio, while the Bottom graph informs about the corresponding $\Delta\theta_0$ chosen by the optimizer. The change of families of solutions as the A/M ratio is clearly visible and it happens in both cases studied. It seems that each of these families has a logarithmic-like behaviour, which is in fact the trend of the overall evolution even despite the change of family of solutions. To investigate this, a least-squares fit of the transfer times of the found optimal solutions to a function of the form

$$f(x) = ae^{-bx+c} + d \tag{17}$$

was performed. Note that the mean radial velocity is recovered by plotting $(R-1)/f(x)$. This quotient is precisely the solid lines one can see in the Top graph of Fig. 11. The change of family of solutions makes the fit difficult to be performed but one observes that the trend of the data fit and the actual data is quite similar. This has been done to justify the following: on the one hand

one can find a value of the A/M ratio for which the minimal radial velocity of 0.55 AU/y can be achieved, but as the A/M ratio increases, the performance of the sailcraft from the mean radial velocity perspective seems to have an asymptotic upper bound: it seems that this propulsion system cannot improve above some threshold that in this case is below the maximal velocity of Earth-Jupiter transfers: 3.82 AU/y.

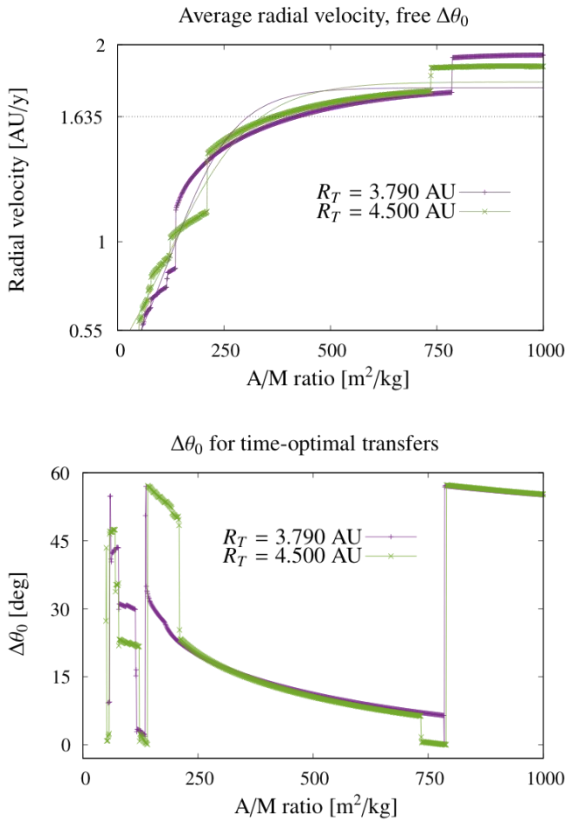

Fig. 11. Top: Mean radial velocity of time-optimal transfers from Earth to the outer Main Belt at $R = 3.790$ and 4.5 AU shown in the radial velocity range (y axis) of previous Earth-Jupiter transfers. Bottom: Initial corresponding $\Delta\theta_0$ of the time-optimal transfers of the Top graph.

The results show that for large enough A/M ratio the transfer times to the inner Main Belt using solely photonic propulsion are of the same order of magnitude as those of classical propulsion means, but not necessarily for transfers to the outer Main Belt, where photonic propulsion systems have an upper boundary of performance. Despite this, for large enough A/M ratio photonic propulsion appears to be a feasible and valuable option as in terms of mean radial velocity it can be compared in some range. The values of the required A/M ratio for which one can achieve the minimum, average and maximal mean radial velocities, extracted from Fig. 10 and 11 Top are summarized in Table 2:

Table 2. Required A/M ratio to transfer from Earth to R AU in the minimum, average and maximal mean radial velocities of classical propulsion systems. "N/A" means Not Applicable.

	Required A/M ratio [m²/kg]			
R [AU]	1.700	1.805	3.790	4.500
0.550 AU/y	N/A	N/A	58.5	50.5
0.620 AU/y	59.5	68.8	N/A	N/A
0.895 AU/y	**96**	**114**	**136.5**	**108**
1.130 AU/y	184.5	224	N/A	N/A
1.635 AU/y	N/A	N/A	420	371
3.820 AU/y	N/A	N/A	-	-

These numbers lead to the following envelope of required SailTrailer A/M ratio, together with their forecasted availability at Sail Assembly (SA) module (using Fig. 7):

- Min: 50.5 m²/kg (forecasted at SA level for 2028)
- **Average: 157.6** m²/kg (forecasted at SA level for 2033)
- Max: 420 m²/kg (forecasted at SA level for 2037)

4.1.3. (Full) Cycler Period

The periods of full cycler trajectories can be easily recovered using the information found above. Denote t_1, t_2, t_3, t_4 the time spans of phases $S \to T$, $T \to T$, $T \to S$ and $S \to S$, respectively. Let us consider a general situation in which the $S \to T$ (unloaded) phase is performed with an effective A/M ratio $\sigma_{S\to T}$. If in the $T \to T$ phase a mass M_{RM} of resource materials is added, the A/M of the loaded SailTrailer is reduced, and depends on $\sigma_{S\to T}$ as follows

$$\sigma_{S\to T} = \left(1 + M_{RM}/M_{ST}\right).\sigma_{T\to S} \qquad (18)$$

Taking this into account, provided one knows both $\sigma_{S\to T}$ and $\sigma_{T\to S}$, and after computing time optimal trajectories as done in the previous subsection, the times t_1 and t_3 are those of the computed trajectories, and the period of the full cycler can be found by just computing the necessary waiting times taking into account t_1 and t_3:

1. First one has to find the minimal time after t_1 so that the relative position of the bodies at the end of the coming back trajectory are satisfied. This is because we want to use the symmetric of the precomputed trajectory. At this instant of time the $T \to S$ phase can start, so one has found $t_1 + t_2$ and t_2 can be deduced.

2. After this, one has to find the minimal time after $t_1 + t_2 + t_3$ so that the relative position of the bodies is that at the very beginning of the precomputed $S \to T$ phase. This quantity is, in fact the period of the full cycler and reads $t_1 + t_2 + t_3 + t_4$, so that the waiting time of the phase $S \to S$, t_4, can be deduced.

As the interest of this paper is to show the performance of SailTrailers that are comparable with other propulsion means, the periods of cyclers with different $\sigma_{S\to T}$ and $\sigma_{T\to S}$ have been computed, but solely among the already computed solutions whose information was already shown in Fig. 10 and 11.

The results concerning the periods of full cyclers can be found in Fig. 12 and 13, that inform about transfers to the inner Main Belt and outer Main Belt, respectively. In each of these graphs the x axis is $\sigma_{S\to T}$, that is, the A/M ratio of the unloaded SailTrailer. The y axis displays a relative measure of how much the Sailcraft is loaded after the $T \to T$ phase, and is measured by

$$\sigma_{T\to S}/\sigma_{S\to T} = 1/\left(1 + M_{RM}/M_{ST}\right) \qquad (19)$$

the quotient between loaded and unloaded A/M ratio, shown as a percentage. Note that the closer $\sigma_{T\to S}$ is to $\sigma_{S\to T}$, the larger is the quotient, and this means that the loaded resource material is low as the A/M ratio of the SailTrailer in the return journey is close to that of the $S \to T$ phase.

Concerning the results to transfer to the inner Main Belt shown in Fig. 12 Top, relating to the travel from 1 AU to 1.7 AU, one observes that the period of the cyclers is similar in all studied cases, except from the top left corner, that starting with the lowest value of the A/M ratio considered, and where the loading is minimal. In the Bottom plot, that corresponds to travelling to 1.805 AU, one observes that these longer periods appear along a curve.

The explanation of this behaviour is, in fact, easy: on the one hand, if one considers a straight horizontal line, that means to fix a relative loading factor, and studies how does the period change as a function of the initial A/M ratio, one expects it to be lower (faster transfer) as the A/M ratio increases, that is, lower as we travel from left to right. On the other hand, if we fix a vertical line, that corresponds to considering a fixed value of the initial A/M ratio and study periods as a function of the relative loading, the lower the loading the lower the period would be (faster transfer again), so that if we travel from bottom to top of the figure, one expects a decrease in the period value.

In the Bottom plot we observe that the transition is not smooth but abrupt. This is because the phasing of the beginning of the $S \to T$ and $T \to S$ may cause the waiting times in the $T \to T$ and $S \to S$ to be longer, and by longer here it means that one has to wait a full synodic period so that the conditions to come back are met again.

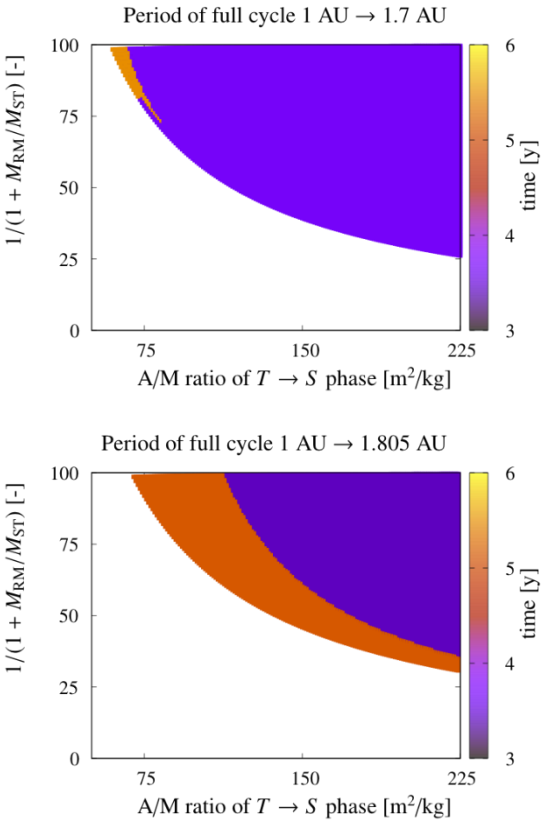

Fig. 12. Full cycle periods for transfers from Earth to the inner Main Belt. The x axis shows the unloaded A/M ratio and the y axis shows the ratio between loaded and unloaded A/M ratios. Top: 1 AU to 1.7 AU. Bottom: 1 AU to 1.805 AU.

In Fig. 13 one can see the results for the transfers to the outer Main Belt, on Top the transfer to 3.790 AU and on the Bottom the transfer to 4.5 AU. The periods of cyclers to these two circles is roughly double the periods of those to the inner Main Belt, so even though the main features of Fig. 12 explained above are also seen here, the longer travel times give rise to a richer structure. Here again the larger periods are those along the boundary that resembles the profile of a $1/x$ function.

Concerning the sudden changes in colour, the length of periods on horizontal and vertical lines from left to right and from bottom to top respectively is no longer monotone as it was in Fig. 12, and this again due to having to wait for longer periods of time (a multiple of the synodic period) that can be attributed to the different initial and final relative phasing of the Earth and the body on the Main Belt.

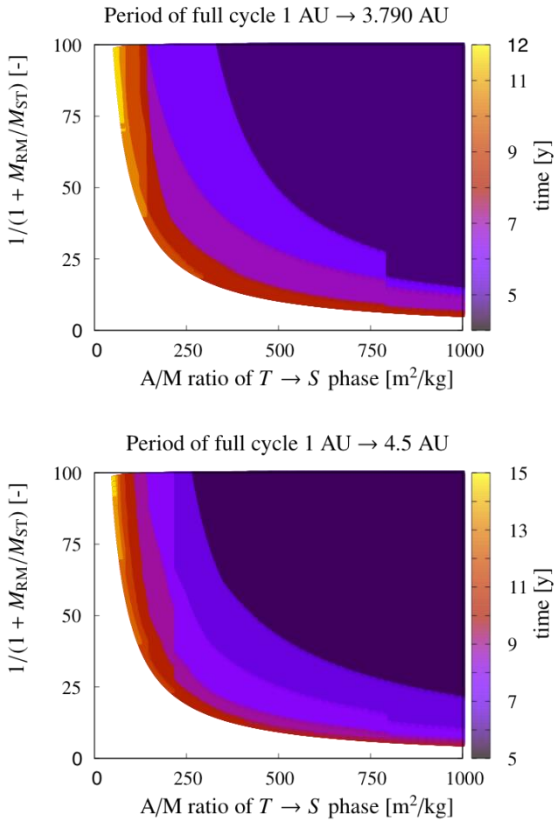

Fig. 13. Full cycle periods for transfers from Earth to the outer Main Belt. The x axis shows the unloaded A/M ratio and the y axis shows the ratio between loaded and unloaded A/M ratios. Top: 1 AU to 3.790 AU. Bottom: 1 AU to 4.5 AU.

5. Conclusions

This paper and the relative work jointly performed by LuxSpace (OHB Group) and the Politecnico di Milano intended helping future "Space Miners" in raising their knowledge about photonic propulsion and thus, in supporting their decision to use (or not) photonic propulsion for Space Resource Businesses.

Focusing on Space Logistics journeys between the Earth and the Main Belt, the paper assessed current solar sail technologies and required advances enabling such missions. The paper also presented the proposed and analysed sail-propelled "Stopover Cyclers" trajectories having cruising speeds similar to those of inter-planetary space probes.

Altogether, the outcomes of this paper formed the basis for our next answers to some first possible "Space Miners" questions to Photonic Propulsion Experts.

5.1. Answers to Future "Space Miners"

The paper indeed posed (and answered) three questions "Space Miners" could ask:

- **Question Q1**: "*Shall we consider photonic propulsion for future (regular) transportation of space resources from the Main Belt (where resource loading will take place) back to Mars, Moon and/or Earth (where unloading will take place) ?*"

  The paper **answered positively** to this question underlining the need for this to continue improving sailcraft technologies and (areal) performances: The sections 2.2 and 4.1.2 assessed that SailTrailers featuring an Area-to-Mass (A/M) ratio of 50 m^2/kg (i.e. one order of magnitude better than the average current technology) could already perform Space Logistic missions at speeds similar to inter-planetary space probes. Such sail technologies could be available around 2028. Lower A/Ms would still enable SailTrailers-based logistic missions, but with longer cycle periods.

- **Question Q2**: "*Could we then take benefit of photonic propulsion to achieve with one sailcraft repeated round trips from the Main Belt back to Mars, Moon and/or Earth for regular load/unload cycles ?*"

  The paper **answered positively** to this question showing that SailTrailers repeating "Stopover Cycles" between starting and target locations will be able to perform this task until their disposal: the analyses performed for section 4 and sub-sections, give rise to a simplified methodology that exploits symmetries of the problem to assess the possibilities of "Stopover Cycler" trajectories as a feasible choice of periodic routes to carry and transport resource materials. The methodology also simplifies the analysis of measuring the effect on the period of such cyclers, of the amount of loaded resource material.

- **Question Q3**: "*Would these photonic propulsion based round trips compete with respect to similar supported by classical propulsions ?*"

  Due to today's lack of information regarding development costs of futuristic, advanced SailTrailers, the paper **could only provide a partial but a priori positive answer** to this question reminding that the SailTrailers here defined will be re-useable and would travel (on average) as fast as past inter-planetary space probes (all using classical propulsion) and this, without any classical propulsive equipment nor propellant. For the same cycle period, SailTrailers plan thus here to substitute propulsive equipment and costly in-space refuellings with valuable space resource materials mass. This for sure will put photonic propulsion as a competitive option for Space Logistics purposes.

5.2. *Concerning the Methodology*

The problem of the design of a stopover cycler trajectory using solar sails with the particularity that the A/M ratio of the back and forth journeys are different has been tackled exploiting the symmetries that are natural for the kind of trajectory this paper has dealt with. This reduction consists of just computing the travels from the starting planet to the target planet for a range of A/M ratios of interest, meaning those that give rise to time-optimal transfers whose mean radial velocity is comparable to those of classical propulsion means.

The period of the full cycles can be easily recovered by first choosing an unloaded and a loaded A/M ratios, and then combining the results to find the waiting times on the starting and target bodies. It is important to note that this requires data of the actual transfer trajectories, namely the travel time and initial and final phasing.

The information on time-optimal trajectories for different values of the A/M ratio of interest can be used to produce maps that inform about the period of the full cycler trajectory as a function of the initial (unloaded) A/M ratio and the relative change in A/M ratio due to the loading of resource materials. In this paper we have provided a methodology to produce such maps, that can be easily reproduced for any starting and target bodies, and for any phasing of interest.

5.3. *Recommendations for Future Works*

The work presented in this paper calls now for further investigations on:

- Sailcraft system design dedicated to SailTrailer missions
- Improvement of sail areal performances, towards the needs expressed by the Breakthrough Starshot Initiative [21]
- Maximal amount of carriable (Space) Resource Material ensuring the controllability of the SailTrailer navigation

Acknowledgments

This paper benefited from the extensive heritage and recent projects relating to the *Sails "Made in Luxembourg" Programme*. Part of this paper is also thanks to the *SpaceResource.lu Initiative from Luxembourg* and to the outstanding work of Professors Michèle Lavagna and Camilla Colombo (co-author) from Politecnico di Milano.

LUXEMBOURG

LET'S MAKE IT HAPPEN

Part of the research leading to these results has received funding from the European Research Council (ERC) under the European Union's Horizon 2020 research and innovation programme as part of project COMPASS (Grant agreement No 679086). The authors acknowledge the use of the Milkyway High Performance Computing Facility, and associated support services at the Politecnico di Milano, in the completion of this work. The use of the computing facilities of the Dynamical Systems Group of the Universitat de Barcelona (Spain) are also acknowledged. The datasets generated for this study can be found in the repository at the link [25].

References

[1] R. L. Forward for Ch. Garner (JPL). Solar Sail Mission Requirements - Final Report. January 12, 2000.

[2] Space Resources.lu: Opportunities for Space Resources Utilization – Future Markets & Value Chains. Study Summary. December 2018.

[3] G. Mengali, A. Quarta. Solar-Sail-Based Stopover Cyclers for Cargo Transportation Missions. *Journal of Spacecraft and Rockets* 2007, 44, 822–830.

[4] F. Dalla Vedova, P. Morin, et al. (LuxSpace), A. Piccinini and N. Ramsden (FANUC). Interfacing Sail Modules for Use with "Space Tugs". (MDPI) Aerospace 2018, 5, 48; doi:10.3390/aerospace5020048.

[5] File:InnerSolarSystem-en.png from Wikipedia. Accessed: 2019-04-26.

[6] Asterank and SpaceReference databases: www.asterank.com and www.spacereference.org. Accessed: 2019-04-26

[7] S. Barton, H. Recht. The Massive Prize Luring Miners to the Stars. www.bloomberg.com/graphics/2018-asteroid-mining. Accessed: 2019-04-26.

[8] SRK Consulting (U.S.). NI 43-101 Technical Report on Updated Resource - Montagne d'Or Gold Deposit, Paul Isnard Project. June 3, 2015.

[9] WWF (France). Montagne d'Or, un mirage économique ? Septembre 2017.

[10] Collectif "Or De Question". Pas d'Or-Pillage en Guyanne. Octobre 2017.

[11] A. Pitoiset. Le Nickel en Nouvelle Calédonie. Maison de la Nouvelle-Calédonie, 2016.

[12] L. L'Huillier and T. Jaffré. (Chapitre 1:) L'Exploitation des Minerais de Nickel en Nouvelle-Calédonie. 2010 (available from ResearchGate).

[13] Le Nickel – SLN (Groupe ERAMET). (Poster:) De la Terre au Métal, le Traitement du Nickel à la SLN.

[14] F. Poulard, X. Daupley, et al. Exploitation Minière et Traitement des Minerais - Tome 6, Février 2017. Collection La Mine en France.

[15] C. Lafleur (March 2010). Costs of US piloted programs. http://www.thespacereview.com/article/1579/1. Accessed: 2018-12-17.

[16] M. Lavagna et al. (Politecnico di Milano). MiNEOs – Executive Summary. July 2018

[17] F. Dalla Vedova, L. Ottone (LuxSpace). DragSail Guidance, Navigation & Control (DGNC) Executive Summary – Dec. 2016. Study performed for ESA (Prime: LuxSpace).

[18] F. Dalla Vedova. LuxSpace contribution to Technical Note 3 "Environmental feedback caused by passive deorbiting

devices" (v2.0, dated: 10/12/2018) of ESA/ESOC contract "Environmental aspects of passive de-orbiting devices" (Prime: Politecnico di Milano)
[19] C. McInnes (University of Strathclyde). Solar Sailing - What are we waiting for? Solar Sail Technologies and Applications Conference. NASA/GSFC 28-29 September 2004
[20] M. Macdonald (University of Glasgow) and C. McInnes (University of Strathclyde). A Near-Term Roadmap for Solar Sailing. IAC-04-U.1.09 Paper for 55th International Astronautical Congress 2004 - Vancouver, Canada
[21] G. Popkin. First Trip to the Stars. Nature, Vol. 542, February 2017.
[22] T.T. McConaghy, R.P. Russell and J.M. Longuski. Toward a Standard Nomenclature for Earth-Mars Cycler Trajectories. Journal of Spacecraft and Rockets, 2005,42, 694-698.
[23] F.L. Markley and J.L. Crassidis. Fundamentals of Spacecraft Attitude Determination and Control. Space Technology Library. Springer New York, 2014.
[24] G. Mengali, and A. Quarta. "Optimal Three-Dimensional Interplanetary Rendezvous Using Nonideal Solar Sail," Journal of Guidance, Control, and Dynamics, Vol. 28, No. 1, Jan.–Feb. 2005, pp. 173–177
[25] COMPASS website: www.compass.polimi.it/ publications